High harmonic generation in crystals using maximally localized Wannier functions

R. E. F. Silva [1,2,*] F. Martín,[3,4,5] and M. Ivanov[1,6,7,†]

[1]*Max-Born-Institut, Max Born Strasse 2A, D-12489 Berlin, Germany*
[2]*Departamento de Física Teórica de la Materia Condensada, Universidad Autónoma de Madrid, E-28049 Madrid, Spain*
[3]*Departamento de Química, Universidad Autónoma de Madrid, 28049 Madrid, Spain*
[4]*Instituto Madrileño de Estudios Avanzados en Nanociencia, 28049 Madrid, Spain*
[5]*Condensed Matter Physics Center (IFIMAC), Universidad Autónoma de Madrid, E-28049 Madrid, Spain*
[6]*Blackett Laboratory, Imperial College London, South Kensington Campus, SW7 2AZ London, United Kingdom*
[7]*Department of Physics, Humboldt University, Newtonstrasse 15, 12489 Berlin, Germany*

In this work, the nonlinear optical response, and in particular, the high harmonic generation of semiconductors, is addressed by using the Wannier gauge. One of the main problems in the time evolution of the Semiconductor Bloch equations resides in the fact that the dipole couplings between different bands can diverge and have a random phase along the reciprocal space, and this leads to numerical instability. To address this problem, we propose the use of the maximally localized Wannier functions that provide a framework to map *ab initio* calculations to an effective tight-binding Hamiltonian with great accuracy. We show that working in the Wannier gauge, the basis set in which the Bloch functions are constructed directly from the Wannier functions, the dipole couplings become smooth along the reciprocal space, thus avoiding the problem of random phases. High harmonic generation is computed for a two-dimensional monolayer of hexagonal boron nitride as a numerical demonstration.

I. INTRODUCTION

Since the discovery of high harmonic generation (HHG) in solids [1], several works demonstrate the potential of analyzing the light emitted by bulk electrons in solids when exposed to intense laser fields. Recent results include the observation of dynamical Bloch oscillations [2,3], band structure tomography [4,5], resolving electron-hole dynamics [6,7], including dynamics in strongly correlated systems and phase transitions in the Mott insulator [8], the Peierls phase transition [6], topological phase transitions in the Haldane model [9], or the imprint of the Berry phase on the high harmonic spectrum [10,11].

The first theoretical works trying to describe HHG in solids are previous to the experimental realization of the process [12,13], but interest in the theoretical understanding had grown in the last years [5,14–20]. Several theoretical approaches were used in this context: solution of the time-dependent Schrödinger equation (TDSE) [17], time-dependent density functional theory (TDDFT) [5], and semiconductor Bloch equations (SBE) [13,21].

Despite the variety of theoretical approaches used up to now, calculation of nonlinear optical properties of crystals presents several difficulties. In the dipole approximation, two different gauges for the electromagnetic field are usually used: length gauge (LG) and velocity gauge (VG). In the VG, the advantage with respect to the LG is that the dynamical

equations become decoupled in the Brillouin zone, but a large number of bands need to be included in the calculation to obtain the converged result [22,23]. On the other hand, the LG gives the converged result for low frequencies with a modest number of bands included in the calculation. In the LG, the problem arises in the representation of the position operator, that now involves a derivative in the Brillouin zone [24]. Evaluating this derivative is a numerical challenge, since the Bloch eigenstates of the crystalline Hamiltonian are defined up to a random phase in the Brillouin zone. In this work we propose a way to circumvent this problem by using the maximally localized Wannier functions (MLWF) that cure this gauge freedom [25,26]. The formalism developed in this work can be applied to analytical tight-binding models, but also for DFT calculations that can be mapped to a tight-binding Hamiltonian using the MLWF procedure [25–27].

In a complete analogy with molecular physics, this work proposes a diabatic basis in which the numerical solution of SBE can be achieved easily—the Wannier gauge [26]. It must be stressed that when one is referring to the LG versus the VG, we are dealing with the intrinsic gauge freedom to describe the electromagnetic field. On the other hand, when we are referring to the Hamiltonian gauge versus the Wannier gauge, we are dealing with two different basis sets in which we can solve our quantum-mechanical problem. The Hamiltonian gauge is a choice of a basis set in which we expand our wave function (or density matrix) in Bloch eigenstates of the crystalline Hamiltonian. On the other hand, the Wannier gauge is the gauge in which calculations are done using an expansion on Bloch states that are constructed from localized Wannier orbitals. In analogy with molecular physics, the Hamiltonian

*ruiefdasilva@gmail.com
†mikhail.ivanov@mbi-berlin.de

gauge is what we would think of as an adiabatic basis, and the Wannier gauge is what we would think of as a diabatic basis.

II. THEORY

In this section, we give a brief overview of the theory of nonlinear optical response in semiconductors. It is worth pointing the reader to the work of Blount [24] and to the work of Ventura *et al.* [23,28], where detailed discussion is given on the difficulties that the position operator presents in a crystal. We derive the dynamical equations for the calculation of the bulk current of a semiconductor when in the presence of an intense laser pulse. We will work in the length gauge under the dipole approximation and neglect electron-electron and electron-phonon interactions.

The novelty of this work relies on the numerical solution of the dynamical equations in a diabatic basis instead of solving them in an adiabatic basis. As it is well known in molecular physics, the study of molecular dynamics is sometimes cumbersome if one chooses to work with an adiabatic basis, especially when one needs to deal with avoided crossings or conical intersections. It is much more appropriate to study molecular dynamics in a diabatic basis, in which nonadiabatic couplings are absent or as small as possible [29]. Two major problems arise when calculating the nonadiabatic couplings in the adiabatic basis: the gauge freedom for choosing the eigenstates of the Hamiltonian up to a random phase and the divergences of the nonadiabatic couplings in the vicinity of the avoided crossings or conical intersections.

A. Single-particle theory

Within the dipole approximation and in the LG, the time-dependent Hamiltonian describing the interaction of an electron in a periodic potential with a laser field is

$$\hat{H}(t) = \hat{H}_0 + |e|\boldsymbol{E}(t) \cdot \hat{\boldsymbol{r}}, \qquad (2.1)$$

$$\hat{H}_0 = \frac{\boldsymbol{p}^2}{2m_e} + U(\boldsymbol{r}), \qquad (2.2)$$

$$U(\boldsymbol{r}) = U(\boldsymbol{r} + \boldsymbol{R}), \qquad (2.3)$$

where $\boldsymbol{E}(t)$ is the electric field, $|e|$ is the elementary charge, m_e is the electron mass, and $\boldsymbol{R}$ is a Bravais lattice vector. Let us consider a set of M localized Wannier orbitals in each cell $w_m(\boldsymbol{r} - \boldsymbol{R}) = \langle \boldsymbol{r}|\boldsymbol{R}m \rangle$. We assume that these Wannier orbitals form an orthonormal basis, i.e., $\langle \boldsymbol{R}'n|\boldsymbol{R}m \rangle = \delta_{n,m}\delta_{\boldsymbol{R}',\boldsymbol{R}}$. Assuming that our system contains N_c unitary cells with periodic boundary conditions, we can define Bloch-like functions from these Wannier orbitals:

$$\big|\psi_{m\boldsymbol{k}}^{(W)}\big\rangle = \frac{1}{\sqrt{N_c}} \sum_{\boldsymbol{R}} e^{i\boldsymbol{k}\cdot\boldsymbol{R}}|\boldsymbol{R}m\rangle, \qquad (2.4)$$

$$\big\langle \boldsymbol{r}\big|\psi_{m\boldsymbol{k}}^{(W)}\big\rangle = \frac{1}{\sqrt{N_c V_c}} e^{i\boldsymbol{k}\cdot\boldsymbol{r}} u_{m\boldsymbol{k}}^{(W)}(\boldsymbol{r}), \qquad (2.5)$$

where V_c is the volume of a unit cell, and $u_{m\boldsymbol{k}}^{(W)}(\boldsymbol{r})$ is the periodic part of the Bloch function.

We are interested in the calculation of nonlinear optical response within the dipole approximation, and for a complete

description of the light-matter interaction it is only necessary to have the knowledge of

$$\langle \mathbf{0}n|\hat{H}_0|\boldsymbol{R}m \rangle, \qquad (2.6)$$

$$\langle \mathbf{0}n|\hat{\boldsymbol{r}}|\boldsymbol{R}m \rangle, \qquad (2.7)$$

where $\hat{H}_0$ is the unperturbed Hamiltonian and $\hat{\boldsymbol{r}}$ is the position operator. These matrix elements can either be calculated from an electronic structure calculation followed by a Wannierization procedure [26] or can be set explicitly by analytical tight-binding models. We can define, as in [30], the Hamiltonian and transition dipole moment (also called Berry connection when $n = m$) matrices in the Wannier gauge as

$$H_{nm}^{(W)}(\boldsymbol{k}) \equiv \sum_{\boldsymbol{R}} e^{i\boldsymbol{k}\cdot\boldsymbol{R}} \langle \mathbf{0}n|\hat{H}_0|\boldsymbol{R}m \rangle, \qquad (2.8)$$

$$A_{nm}^{(W)}(\boldsymbol{k}) \equiv \sum_{\boldsymbol{R}} e^{i\boldsymbol{k}\cdot\boldsymbol{R}} \langle \mathbf{0}n|\hat{\boldsymbol{r}}|\boldsymbol{R}m \rangle, \qquad (2.9)$$

where the sum in $\boldsymbol{R}$ runs over all lattice vectors in our system, and the superscript (W) refers to the Wannier gauge (as in [30]). As it will be seen later, these matrices enter in the dynamical equations of our system. Since we are working under the assumption that the Wannier orbitals are localized functions, we expect that the terms $\langle \mathbf{0}n|\hat{H}_0|\boldsymbol{R}m \rangle$ and $\langle \mathbf{0}n|\hat{\boldsymbol{r}}|\boldsymbol{R}m \rangle$ in the sum will decay exponentially with $\boldsymbol{R}$, and this fact will lead to smooth matrices, $H^{(W)}(\boldsymbol{k})$ and $A^{(W)}(\boldsymbol{k})$.

We can write the single-particle unperturbed Hamiltonian as

$$\hat{H}_0 = \sum_{\boldsymbol{k} \in FBZ} \sum_{n,m} H_{nm}^{(W)}(\boldsymbol{k}) \big|\psi_{n\boldsymbol{k}}^{(W)}\big\rangle\big\langle\psi_{m\boldsymbol{k}}^{(W)}\big|, \qquad (2.10)$$

where the sum over $\boldsymbol{k}$ runs over all allowed crystal momentum inside the first Brillouin zone (FBZ). We can work in the basis where $\hat{H}_0$ is diagonal, and for that we only need to diagonalize the $H_{nm}^{(W)}(\boldsymbol{k})$ matrix. We will refer to this basis as the Hamiltonian gauge using the superscript (H). Whenever none of the superscripts are used it means that the result is valid for both (W) and (H) gauges. Both bases are related to each other by a unitary transformation

$$\big|\psi_{n\boldsymbol{k}}^{(H)}\big\rangle = \sum_{m} U_{mn}(\boldsymbol{k})\big|\psi_{m\boldsymbol{k}}^{(W)}\big\rangle, \qquad (2.11)$$

where $U(\boldsymbol{k})$ is a unitary matrix that diagonalizes $H^{(W)}(\boldsymbol{k})$:

$$U^{\dagger}(\boldsymbol{k})H^{(W)}(\boldsymbol{k})U(\boldsymbol{k}) = H^{(H)}(\boldsymbol{k}). \qquad (2.12)$$

The relationship between the $A(\boldsymbol{k})$ matrix in both gauges is [30]

$$A^{(H)}(\boldsymbol{k}) = U^{\dagger}(\boldsymbol{k})A^{(W)}(\boldsymbol{k})U(\boldsymbol{k}) + iU^{\dagger}(\boldsymbol{k})\frac{\partial}{\partial\boldsymbol{k}}U(\boldsymbol{k}). \qquad (2.13)$$

It must be noted that the matrix $U(\boldsymbol{k})$ is not unique. This fact lies on the gauge freedom that we have to choose a global phase for the eigenstates, $|\psi_{n\boldsymbol{k}}^{(H)}\rangle \rightarrow e^{i\theta_n(\boldsymbol{k})}|\psi_{n\boldsymbol{k}}^{(H)}\rangle$. Since the last term, $iU^{\dagger}(\boldsymbol{k})\frac{\partial}{\partial\boldsymbol{k}}U(\boldsymbol{k})$, is not invariant under this phase transformation, we have an intrinsic gauge freedom in the calculation of $A^{(H)}(\boldsymbol{k})$. It is precisely this gauge freedom that we try to avoid using the Wannier gauge.

The matrix elements of the position operator in a finite-volume system with periodic boundary conditions are ill

defined but can be computed in the thermodynamic limit. The representation of the position operator in a Bloch basis is [23,24]

$$\hat{r} = i\frac{\partial}{\partial \boldsymbol{k}} + \hat{A}, \tag{2.14}$$

where $\hat{A}$ is the transition dipole moment, which is defined as

$$A_{nm}(\boldsymbol{k}) = i\int_{V_C} d^D\boldsymbol{r}(u_{nk}(\boldsymbol{r}))^*\frac{\partial}{\partial \boldsymbol{k}}u_{mk}(\boldsymbol{r}). \tag{2.15}$$

In the Wannier gauge the transition dipole moment will be the one defined in Eq. (2.9).

The matrix representation of the current operator in a Bloch basis is defined as

$$\hat{J} = \frac{-|e|}{i\hbar}[\hat{r}, \hat{H}(t)], \tag{2.16}$$

$$(\hat{J})_{\boldsymbol{k},nm} = \frac{-|e|}{\hbar}\left(\frac{\partial}{\partial \boldsymbol{k}}H_{nm}(\boldsymbol{k}) - i[A(\boldsymbol{k}), H(\boldsymbol{k})]_{nm}\right). \tag{2.17}$$

In the Hamiltonian gauge, we can identify the two terms in the expression for the current as the *intraband* and *interband* current:

$$(\hat{J}_{\text{intra}})_{\boldsymbol{k},nm} = \frac{-|e|}{\hbar}\left(\frac{\partial}{\partial \boldsymbol{k}}H_{nm}^{(H)}(\boldsymbol{k})\right), \tag{2.18}$$

$$(\hat{J}_{\text{inter}})_{\boldsymbol{k},nm} = \frac{i|e|}{\hbar}([A^{(H)}(\boldsymbol{k}), H^{(H)}(\boldsymbol{k})]_{nm}). \tag{2.19}$$

It must be emphasized that *intraband* and *interband* currents are gauge-dependent quantities, i.e., they are not physical observables [31,32]. Nevertheless, in the length gauge for the electromagnetic field and in the Hamiltonian gauge, this separation of the current in the *interband* and *intraband* parts provides us physical insight.

B. Many-body theory

Having all the relevant operators (the current and the time-dependent Hamiltonian operator) defined in first quantization, we proceed to define all the relevant operators in a second quantization formalism. The time-dependent many-body Hamiltonian is just

$$\hat{\mathcal{H}}(t) = \sum_{\boldsymbol{k}\in FBZ}\sum_{n,m}c_{nk}^{\dagger}H_{nm}(\boldsymbol{k})c_{mk}$$
$$+ \sum_{\boldsymbol{k}\in FBZ}\sum_{n,m}c_{nk}^{\dagger}|e|\boldsymbol{E}(t)\cdot\left[i\delta_{nm}\frac{\partial}{\partial \boldsymbol{k}} + A_{nm}(\boldsymbol{k})\right]c_{mk}, \tag{2.20}$$

where $c_{nk}^{\dagger}$ (c_{nk}) is the fermionic creation (annihilation) operator of a Bloch state. The many-body current operator can also be expressed as

$$\hat{\mathcal{J}} = \sum_{\boldsymbol{k}\in FBZ}\sum_{n,m}(\hat{J})_{\boldsymbol{k},nm}c_{nk}^{\dagger}c_{mk}, \tag{2.21}$$

$$= \sum_{\boldsymbol{k}\in FBZ}\sum_{n,m}\frac{-|e|}{\hbar}\left(\frac{\partial}{\partial \boldsymbol{k}}H_{nm}(\boldsymbol{k})\right)c_{nk}^{\dagger}c_{mk}$$
$$+ \sum_{\boldsymbol{k}\in FBZ}\sum_{n,m}\frac{i|e|}{\hbar}[A(\boldsymbol{k}), H(\boldsymbol{k})]_{nm}c_{nk}^{\dagger}c_{mk}. \tag{2.22}$$

The observable that we are interested in is the mean value of the current operator, $\langle\hat{\mathcal{J}}\rangle$, and for that we need to know only the mean values of $c_{nk}^{\dagger}c_{mk}$. Let us define the reduced density matrix (RDM) as

$$\rho_{nm}(\boldsymbol{k}, t) = \langle c_{mk}^{\dagger}c_{nk}\rangle. \tag{2.23}$$

Note that the band indexes are switched. The equations of motion for the RDM have the following form [23]:

$$i\hbar\frac{\partial}{\partial t}\rho_{nm}(\boldsymbol{k}, t) = \langle[c_{mk}^{\dagger}c_{nk}, \hat{\mathcal{H}}(t)]\rangle$$
$$= [H(\boldsymbol{k}), \rho(\boldsymbol{k}, t)]_{nm}$$
$$+ i|e|\boldsymbol{E}(t)\cdot\frac{\partial}{\partial \boldsymbol{k}}\rho_{nm}(\boldsymbol{k}, t)$$
$$+ |e|\boldsymbol{E}(t)\cdot[A(\boldsymbol{k}), \rho(\boldsymbol{k}, t)]_{nm}. \tag{2.24}$$

With these equations we have the complete set of dynamical equations for our problem. It is precisely when we look at the structure of the equations of motion for the RDM that we can appreciate the advantage of using the Wannier gauge. Since the Wannier gauge provides smooth $A(\boldsymbol{k})$ and $H(\boldsymbol{k})$, the numerical propagation of the equations of motion in a discretized $\boldsymbol{k}$ grid is easier compared to the Hamiltonian gauge case.

C. Initial conditions

We can assume that the electrons in a solid are in thermal equilibrium before the application of a coherent perturbation. Thus our initial state is a mixed state without coherence between eigenstates with a Fermi-Dirac distribution. We can construct the unperturbed RDM in the (H) gauge,

$$\rho_{nm}^{(H)}(\boldsymbol{k}, t_0) = \delta_{nm}s_np_{nk}, \tag{2.25}$$

where $s_n = 1, 2$ takes into account spin degeneracy, $p_{nk} = 1/(e^{[(\varepsilon_n(\boldsymbol{k})-\mu)/k_BT]})$, and μ is the chemical potential. The relationship between the two RDM in both gauges is given by

$$\rho_{nm}^{(H)}(\boldsymbol{k}, t) = \sum_{ab}U_{nb}^{\dagger}(\boldsymbol{k})\rho_{ba}^{(W)}(\boldsymbol{k}, t)U_{am}(\boldsymbol{k}), \tag{2.26}$$

$$\rho_{nm}^{(W)}(\boldsymbol{k}, t) = \sum_{ab}U_{nb}(\boldsymbol{k})\rho_{ba}^{(H)}(\boldsymbol{k}, t)U_{am}^{\dagger}(\boldsymbol{k}). \tag{2.27}$$

Since the initial state at t_0 does not have any coherence (i.e., when $n \neq m$, $\langle c_{mk}^{(H)\dagger}c_{nk}^{(H)}\rangle = 0$), the gauge freedom in the choice of U will not change $\rho_{nm}^{(W)}(\boldsymbol{k}, t_0)$. This makes our initial RDM in the Wannier gauge robust under phase transformations.

D. Dephasing

For a proper modeling of the HHG process, decoherence due to electron-electron or electron-phonon scattering must be taken into account. In this work, we will introduce decoherence in the same way it was introduced by Vampa *et al.* [15] in the Hamiltonian gauge. There is an ongoing debate about the origin of the very short dephasing times needed to obtain agreement with the experimental results ($T_2 \approx 2$ fs) [15]. Recently, the importance of propagation effects in solids was pointed out in [19]. The dynamical equation for the RDM
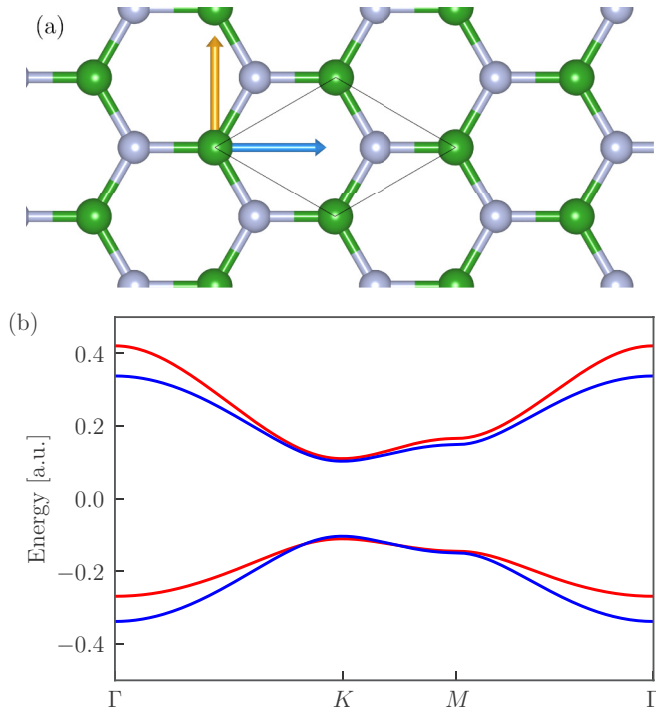
FIG. 1. (a) Single layer of hexagonal boron nitride. The boron (nitrogen) atoms are in green (gray). The blue (yellow) arrow represents the laser polarization along $\Gamma - M$ ($\Gamma - K$). (b) Electronic band structure for the effective model (blue line) and for the *ab initio* model (red line).

in the Hamiltonian gauge, including dephasing, will now take the form

$$i\hbar \frac{\partial}{\partial t} \rho_{nm}^{(H)}(\boldsymbol{k}, t) = [H^{(H)}(\boldsymbol{k}), \rho^{(H)}(\boldsymbol{k}, t)]_{nm}$$

$$+ i|e|\boldsymbol{E}(t) \cdot \frac{\partial}{\partial \boldsymbol{k}} \rho_{nm}^{(H)}(\boldsymbol{k}, t)$$

$$+ |e|\boldsymbol{E}(t) \cdot [\boldsymbol{A}^{(H)}(\boldsymbol{k}), \rho^{(H)}(\boldsymbol{k}, t)]_{nm}$$

$$- i\hbar \frac{(1 - \delta_{nm})}{T_2} \rho_{nm}^{(H)}(\boldsymbol{k}, t). \qquad (2.28)$$

The dephasing term in the equation of motion for the RDM is better to be handled in the Hamiltonian gauge. In practice, to solve this set of equations numerically we propagate the coherent part of the equation in the Wannier gauge and the dephasing term is introduced in the Hamiltonian gauge.

III. NUMERICAL RESULTS

In this section, we will show the results of applying the formalism developed to the case of a single monolayer of hexagonal boron nitride (hBN). In Fig. 1(a), we show the hexagonal structure of the hBN and the two laser polarizations that will be used in this work, along the $\Gamma - M$ and $\Gamma - K$ directions. The distance between neighbor atoms is 1.446 Å.

We will use two different sets of parameters for the Hamiltonian and dipole couplings. The first parametrization is the widely used simple tight-binding model in which only p_z orbitals are considered [33]. We set the hopping constant t_0 to be 2.92 eV and the on-site energy of the two different atoms to be $\varepsilon_B = -\varepsilon_N = 2.81$ eV. For the position operator we assume
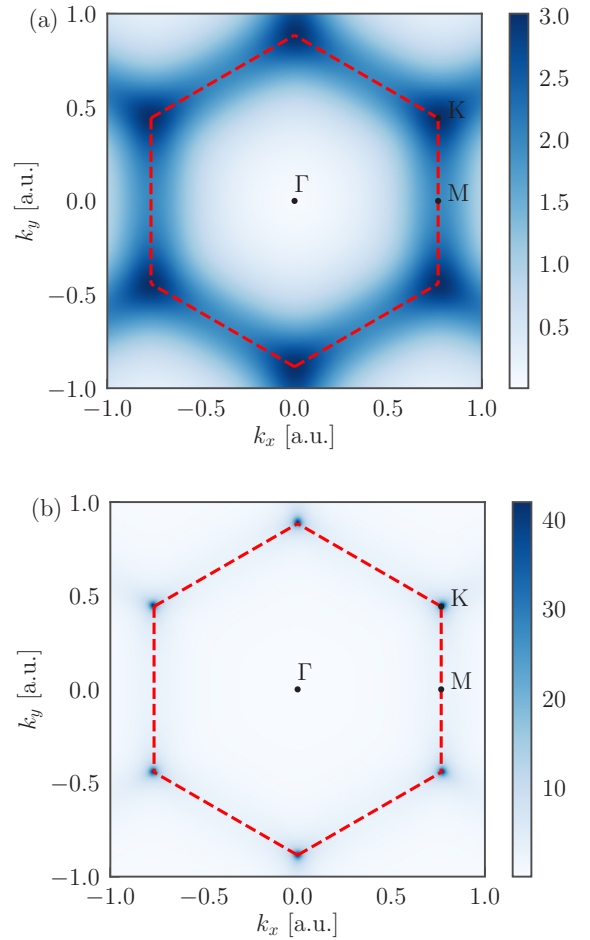

FIG. 2. (a) Transition dipole moment between the valence band and the conduction band, $|A_{vc}^{(H)}(\boldsymbol{k})| = \sqrt{|A_{x,vc}^{(H)}(\boldsymbol{k})|^2 + |A_{y,vc}^{(H)}(\boldsymbol{k})|^2}$, for the effective model. (b) Same as in (a) but for $\varepsilon_B = -\varepsilon_N = 0.2$ eV.

that it is diagonal in the basis of the localized Wannier orbitals, i.e.,

$$\langle \boldsymbol{0}n|\hat{\boldsymbol{r}}|\boldsymbol{R}m \rangle = \delta_{nm}\delta_{\boldsymbol{0}\boldsymbol{R}}\boldsymbol{\tau}_n, \qquad (3.1)$$

where $\boldsymbol{\tau}_n$ is the center of the n Wannier function. We will refer to this parametrization as the effective model. The second parametrization is done by performing an *ab initio* calculation using the HSE06 functional and a 10×10 Monkhorst-Pack grid using the QUANTUM ESPRESSO code [34]. We perform a projection on the p_z orbitals and a Wannierization procedure to obtain the Hamiltonian and dipole couplings using the WANNIER90 software [35]. We refer to this parametrization as the *ab initio* model. In Fig. 1(b) we show the electronic band structure for both models.

In order to emphasize the necessity of employing the Wannier gauge for the numerical computation of the nonlinear optical properties, we show in Fig. 2(a) the transition dipole moment between the valence and the conduction band. It is clear that the transition dipole moment is centered around the K and K' points, and when the on-site energy of the atoms goes to smaller values, see Fig. 2(b), the transition dipole moment becomes more peaked. To properly describe these abrupt changes in the Brillouin zone using the Hamiltonian
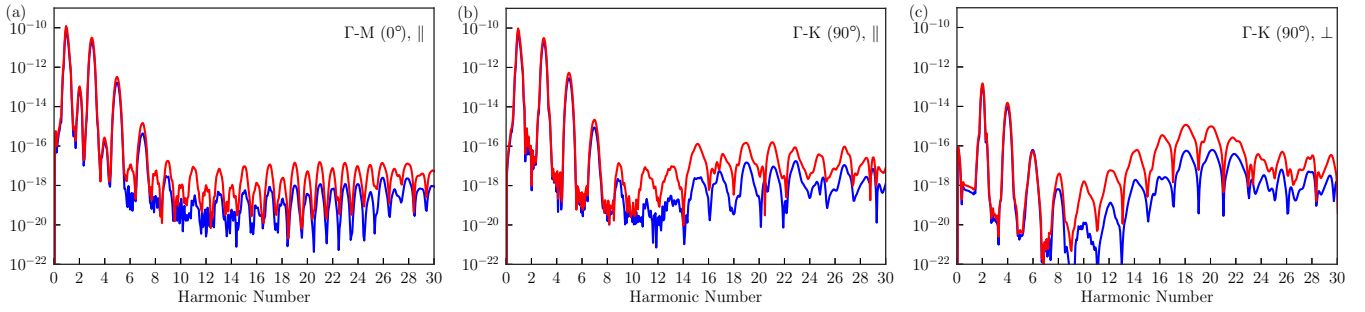
FIG. 3. High harmonic generation spectrum computed for a single monolayer of hBN for the effective model (blue lines) and for the *ab-initio* model (red lines). (a,b,c) Harmonic spectrum for a laser pulse in the $\Gamma - M$ ($\Gamma - K$, $\Gamma - K$) direction along its parallel (parallel, perpendicular) direction, respectively.

gauge requires a very fine grid in k space. On the other hand, in the Wannier gauge the Bloch functions are defined to be smooth and continuous in the reciprocal space. Another advantage of using the Wannier gauge is that in the case of using an *ab initio* calculation we can circumvent the problem of random phases, which was pointed out as a major theoretical challenge [36,37].

The laser pulse has a peak field of 40 MV/cm, a wavelength of 3 μm, and 34.2 fs of FWHM in intensity with a $\cos^2$ envelope. We solve the equation of motion for the RDM using a 300×300 Monkhorst-Pack grid and propagating with a fourth-order Runge-Kutta propagator with a time step of 2.5 as. For all calculations, we have used a dephasing time, T_2, of 2 fs. Two different polarizations for the electric field of the laser pulse are used, along the $\Gamma - M$ ($0°$) and along the $\Gamma - K$ ($90°$) direction. The HHG spectrum is evaluated along the parallel ($\parallel$) and perpendicular ($\perp$) direction of the laser pulse and it is calculated as the power spectrum of the expectation value of the dipole acceleration.

In Fig. 3 is shown the spectrum for different pulse directions and different directions of emission. Symmetry imposes that for the $\Gamma - M$ direction of the laser pulse the perpendicular current is strictly zero and for that reason is not shown. On the other hand, for the parallel emission, both even and odd harmonics are allowed due to the breaking of the inversion symmetry. When the laser pulse is aligned along the $\Gamma - K$ direction, symmetry restricts harmonic emission to odd (even) harmonics for the parallel (perpendicular) emission [38]. It is clear that first-order harmonics, which are generated mostly by intraband current [15], have an exponential decay until harmonic 13, which approximately corresponds to the band-gap energy, 5.62 eV. It can be observed that the agreement between both models is extremely good given the simplicity of the effective model. For intraband harmonics the agreement between both approaches is almost quantitative, and for harmonics higher than the band-gap energy, usually coming from interband polarizations, the results agree on the overall shape having a discrepancy in its absolute value.

The quantitative discrepancy in the region of interband harmonics arises due to the approximation done in the construction of the dipole operator in the effective model. The assumption made in Eq. (3.1) for the effective model strongly reduces the possibility of recombination between distant Wannier orbitals, and this can be observed by looking at the suppression of high harmonics when comparing against the *ab initio* model. Furthermore, the low-order harmonics have a much better agreement, since it is not expected that recombination elements have a strong influence on them, just like Brunel harmonics in atomic HHG.

IV. CONCLUSION

The Wannier gauge is presented in this work as a way to avoid the problem of random phases of the dipole couplings along the FBZ. The dynamical equations for the RDM are derived in the Wannier gauge. The presented formalism can provide a new framework in which DFT calculations and simple tight-binding Hamiltonians can be used for the description of the HHG process. The harmonic spectrum for a single monolayer of hBN is calculated, and the results validate the use of the simplest tight-binding Hamiltonian commonly used [33] to study HHG when compared to *ab initio* DFT calculations. Our work opens a window for the calculation of nonlinear optical response in crystals by using parameters directly extracted from *ab initio* calculations using the MLWF procedure, which up to now was a cumbersome task due to the problem of random phases in the dipole couplings.

[1] S. Ghimire, A. D. DiChiara, E. Sistrunk, P. Agostini, L. F. DiMauro, and D. A. Reis, Nat. Phys. **7**, 138 (2011).

[2] O. Schubert, M. Hohenleutner, F. Langer, B. Urbanek, C. Lange, U. Huttner, D. Golde, T. Meier, M. Kira, S. W. Koch *et al.*, Nat. Photonics **8**, 119 (2014).

[3] T. T. Luu, M. Garg, S. Y. Kruchinin, A. Moulet, M. T. Hassan, and E. Goulielmakis, Nature (London) **521**, 498 (2015).

[4] G. Vampa, T. J. Hammond, N. Thiré, B. E. Schmidt, F. Légaré, C. R. McDonald, T. Brabec, D. D. Klug, and P. B. Corkum, Phys. Rev. Lett. **115**, 193603 (2015).

[5] N. Tancogne-Dejean, O. D. Mücke, F. X. Kärtner, and A. Rubio, Nat. Commun. **8**, 745 (2017).

[6] D. Bauer and K. K. Hansen, Phys. Rev. Lett. **120**, 177401 (2018).

[7] C. R. McDonald, G. Vampa, P. B. Corkum, and T. Brabec, Phys. Rev. A **92**, 033845 (2015).

[8] R. E. F. Silva, I. V. Blinov, A. N. Rubtsov, O. Smirnova, and M. Ivanov, Nat. Photonics **12**, 266 (2018).

[9] R. E. F. Silva, Á. Jiménez-Galán, B. Amorim, O. Smirnova, and M. Ivanov, Nat. Photon. (2019), doi: 10.1038/s41566-019-0516-1.

[10] T. T. Luu and H. J. Wörner, Nat. Commun. **9**, 916 (2018).

[11] H. Liu, Y. Li, Y. S. You, S. Ghimire, T. F. Heinz, and D. A. Reis, Nat. Phys. **13**, 262 (2017).

[12] L. Plaja and L. Roso-Franco, Phys. Rev. B **45**, 8334 (1992).

[13] D. Golde, T. Meier, and S. W. Koch, Phys. Rev. B **77**, 075330 (2008).

[14] P. G. Hawkins and M. Y. Ivanov, Phys. Rev. A **87**, 063842 (2013).

[15] G. Vampa, C. R. McDonald, G. Orlando, D. D. Klug, P. B. Corkum, and T. Brabec, Phys. Rev. Lett. **113**, 073901 (2014).

[16] P. G. Hawkins, M. Y. Ivanov, and V. S. Yakovlev, Phys. Rev. A **91**, 013405 (2015).

[17] M. Korbman, S. Y. Kruchinin, and V. S. Yakovlev, New J. Phys. **15**, 013006 (2013).

[18] M. S. Wismer, S. Y. Kruchinin, M. Ciappina, M. I. Stockman, and V. S. Yakovlev, Phys. Rev. Lett. **116**, 197401 (2016).

[19] I. Floss, C. Lemell, G. Wachter, V. Smejkal, S. A. Sato, X.-M. Tong, K. Yabana, and J. Burgdörfer, Phys. Rev. A **97**, 011401(R) (2018).

[20] E. N. Osika, A. Chacón, L. Ortmann, N. Suárez, J. A. Pérez-Hernández, B. Szafran, M. F. Ciappina, F. Sols, A. S. Landsman, and M. Lewenstein, Phys. Rev. X **7**, 021017 (2017).

[21] M. Kira and S. W. Koch, *Semiconductor Quantum Optics* (Cambridge University Press, Cambridge, UK, 2012).

[22] C. Aversa and J. E. Sipe, Phys. Rev. B **52**, 14636 (1995).

[23] G. B. Ventura, D. J. Passos, J. M. B Lopes dos Santos, J. M. Viana Parente Lopes, and N. M. R. Peres, Phys. Rev. B **96**, 035431 (2017).

[24] E. Blount, Solid State Phys. **13**, 305 (1962).

[25] N. Marzari and D. Vanderbilt, Phys. Rev. B **56**, 12847 (1997).

[26] N. Marzari, A. A. Mostofi, J. R. Yates, I. Souza, and D. Vanderbilt, Rev. Mod. Phys. **84**, 1419 (2012).

[27] A. A. Mostofi, J. R. Yates, G. Pizzi, Y.-S. Lee, I. Souza, D. Vanderbilt, and N. Marzari, Comput. Phys. Commun. **185**, 2309 (2014).

[28] G. B. Ventura, Master's thesis, Faculdade de Ciências da Universidade do Porto, 2016.

[29] D. J. Tannor, *Introduction to Quantum Mechanics: A Time-Dependent Perspective* (University Science Books, Sausalito, CA, 2006).

[30] X. Wang, J. R. Yates, I. Souza, and D. Vanderbilt, Phys. Rev. B **74**, 195118 (2006).

[31] P. Földi, Phys. Rev. B **96**, 035112 (2017).

[32] G. Ernotte, T. Hammond, and M. Taucer, Phys. Rev. B **98**, 235202 (2018).

[33] A. H. Castro Neto, F. Guinea, N. M. R. Peres, K. S. Novoselov, and A. K. Geim, Rev. Mod. Phys. **81**, 109 (2009).

[34] P. Giannozzi, S. Baroni, N. Bonini, M. Calandra, R. Car, C. Cavazzoni, D. Ceresoli, G. L. Chiarotti, M. Cococcioni, I. Dabo *et al.*, J. Phys.: Condens. Matter **21**, 395502 (2009).

[35] A. A. Mostofi, J. R. Yates, Y.-S. Lee, I. Souza, D. Vanderbilt, and N. Marzari, Comput. Phys. Commun. **178**, 685 (2008).

[36] S. Jiang, J. Chen, H. Wei, C. Yu, R. Lu, and C. D. Lin, Phys. Rev. Lett. **120**, 253201 (2018).

[37] C. Yu, S. Jiang, and R. Lu, Adv. Phys.: X **4**, 1562982 (2019).

[38] Y. S. You, D. A. Reis, and S. Ghimire, Nat. Phys. **13**, 345 (2017).